Data in Brief 57 (2024) 110905

Contents lists available at ScienceDirect

Data in Brief

journal homepage: www.elsevier.com/locate/dib

Data Article

Data of crystal structure of the monomeric red fluorescent protein DsRed

Ki Hyun Nam

College of General Education, Kookmin University, Seoul 02707, Republic of Korea

ARTICLE INFO

Article history:
Received 8 August 2024
Revised 27 August 2024
Accepted 28 August 2024
Available online 5 September 2024

Dataset link: Crystal structure of DsRed-Monomer (Original data)

Keywords:
Substrate binding protein
Single domain
Structural flexibility
X-ray diffraction data
Crystal structure

ABSTRACT

The monomeric red fluorescent protein DsRed (mDsRed) is an optical probe widely used in multicolor applications in flow cytometry and fluorescence microscopy. Although the crystal structure of monomeric DsRed has been determined, its molecular dynamics have not been fully elucidated. To better understand its molecular flexibility, the crystal structure of mDsRed was recently determined, and its structure and temperature factors were analyzed. Solvent-accessible hole connected with the mDsRed chromophore was observed on the mDsRed surface structure. Electron density map analysis showed the tyrosine-ring group of the mDsRed chromophore in a *cis*-conformation, exhibiting flexibility with a nonplanar configuration between the tyrosine and imidazoline rings of the chromophore. Temperature factor analysis indicated that the top and bottom of the β-barrel are relatively flexible. These structural findings extended our understanding of the molecular flexibility of mDsRed. The detailed data collection and structure determination reported in this study can be used for future structural analyses.

E-mail address: structure@kookmin.ac.kr

https://doi.org/10.1016/j.dib.2024.110905

Specifications Table

Subject	Biological science
Specific subject area	Structural Biology
Type of data	Processed
Data collection	Synchrotron: Pohang Light Source II (PLS-II) Beamline: 7C Detector: Q270 CCD X-ray detector (ADSC, USA) Data collection energy: 14.82 keV Data collection temperature: 100 K Data processing program: HKL2000
Data source location	Institution: Kookmin University City/Town/Region: Seoul Country: Republic of Korea
Data accessibility	Structure factor and coordinates Repository name: Protein Data Bank Data identification number: https://doi.org/10.2210/pdb8WGP/pdb Direct URL to data: https://www.rcsb.org/structure/8WGP Instructions for accessing these data: Coordinate and structure factor can be download without permission.
Related research article	K.H. Nam, Structural Flexibility of the Monomeric Red Fluorescent Protein DsRed. Crystals 14 (1), 62; https://doi.org/10.3390/cryst14010062 [1].

1. Value of The Data

- These data provide the coordinates and structure factors of mDsRed to aid in understanding its molecular function.
- These data offer useful information about the flexibility of the mDsRed chromophore in its nonplanar configuration, which contributes to the understanding of the molecular dynamics of fluorescent proteins (FPs).
- These data show distinct temperature factors compared to the previously determined mDsRed structure, providing insights into the molecular flexibility of mDsRed.
- These data can be used to engineer FPs to improve their fluorescence properties.

2. Background

Fluorescent proteins are widely used as optical probes in molecular and cellular biology and as biosensor probes for detecting metal ions and pH levels [2–6]. The original tetrameric DsRed, derived from the reef coral *Dendronephthya* sp., was engineered into monomeric DsRed (mDsRed) to avoid slow maturation and challenges in FRET applications [7–10]. mDsRed is widely used in multicolor applications such as flow cytometry and fluorescence microscopy [11]. The overall structure of mDsRed has been reported, providing useful information for understanding the structural properties of mDsRed [10]. However, the structural dynamics of mDsRed have not been fully elucidated. To understand the fundamental properties of mDsRed, recent studies have analyzed the structural dynamics of mDsRed using new crystal structures [1]. In this study, the detailed data collection and structure determination of mDsRed are reported for future utilization of the mDsRed structure.

3. Data Description

The indexing results of X-ray diffraction (XRD) experiments showed that rod-shaped mDsRed crystals belonged to the monoclinic space group $P2_1$. The unit cell dimensions of mDsRed were a = 39.56 Å, b = 107.00 Å, c = 50.02 Å, and β = 104.86° (Table 1). Matthews coefficient analysis

Table 1
Data collection statistics for mDsRed

Data collection	mDsRed
X-ray energy (eV)	14820
Space group	$P2_1$
Cell dimension	
a, b, c (Å)	39.56, 107.00, 50.02
α, β, γ (°)	90.00, 104.86, 90.00
Resolution (Å)	50.0–2.90 (2.95–2.90)
Unique reflections	8136 (362)
Completeness (%)	91.5 (80.6)
Multiplicity	2.8 (2.1)
I/sigma	36.47 (5.63)
R_{merge}	0.157 (0.354)
R_{meas}	0.152 (0.441)
R_{pim}	0.261 (0.102)
CC1/2	0.929 (0.646)
CC*	0.980 (0.886)

Values for the outer shell are given in parentheses.

showed that two mDsRed molecules occupied an asymmetric unit, with a VM of 2.11 Å³/Da and a solvent content of 41.84%. XRD data were processed in the range of 50.0–2.9 Å resolution, with 8,136 unique reflections. The overall completeness, redundancy, and I/σ of mDsRed were 91.5%, 2.8, and 12.62, respectively. The overall I/σ, R_{merge}, R_{meas}, R_{pim}, CC1/2, and CC* values of mDsRed XRD data were 12.62, 0.157, 0.152, 0.188, 0.929, and 0.980, respectively (Fig. 1). At low (50.00–7.86 Å) resolution, the I/σ, R_{merge}, R_{meas}, R_{pim}, CC1/2, and CC* values were 30.16, 0.090, 0.107, 0.056, 0.990, and 0.998, respectively. At high (2.95–2.90 Å) resolution, the I/σ, R_{merge}, R_{meas}, R_{pim}, CC1/2, and CC* values were 4.04, 0.354, 0.443, 0.261, 0.646, and 0.886, respectively.

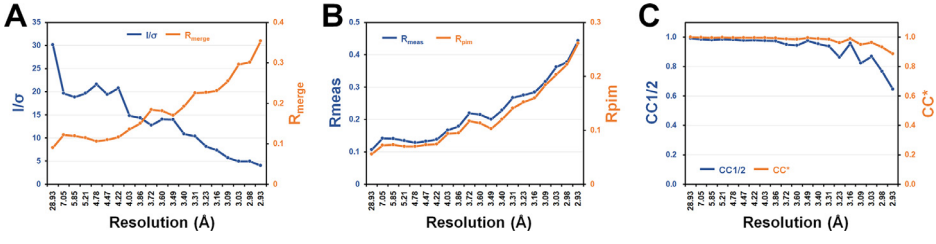

Fig. 1. Data processing results of mDsRed for (A) I/σ and R_{merge}, (B) R_{meas} and $R_{pim,}$ and (C) CC1/2 and CC*.

The phasing problem of mDsRed was solved using the molecular replacement method. The electron density map was suitable for model building for all residues. The resolution of the final refinement of the mDsRed structure was 26.10 to 2.90 Å, with a completeness of 90.7%. A total of 7,733 reflections were used in refinement, with a free R-value test set count of 388. The R_{work} (working + test set), R_{work} (working set), and R_{free} values of the final structure of mDsRed were 0.199, 0.197, and 0.242, respectively (Table 2). A total of 3,510 protein atoms without hydrogen and 44 water molecules were defined. The correlation coefficients Fo-Fc and Fo-Fc free were 0.903 and 0.856, respectively. The RMS deviation of bond lengths and angles were 0.011 and 1.680, respectively.

Ramachandran analysis of the deposited mDsRed showed that 388 and 33 of 427 residues were in the favored (90.9%) and allowed (7.7%) regions, respectively (Fig. 2). Meanwhile, Lys50 (phi, psi: 157.6, 114.8), Pro190 (−64.5, −136.7), and Asn192 (−59.2, 97.1) from chain A and Glu5 (−35.0, −31.6), Glu34 (170.1, 147.5), and Lys50 (166.4, 126.2) from chain B were in the outlier (1.4%) region (Fig. 2).

Table 2
Refinement statistics for mDsRed.

Refinement	mDsRed
Resolution (Å)	26.10–2.90
R_{work} [a]	0.197
R_{free} [b]	0.242
RMS deviations	
Bonds (Å)	0.011
Angles (°)	1.680
B factors (Å^2)	
Protein	13.50
Chromophore	25.53
Ramachandran plot	
Favored (%)	90.5
Allowed (%)	7.9
Disallowed (%)	1.6

[a] $R_{work} = \Sigma||Fobs| \Sigma |Fcalc||/\Sigma|Fobs|$, where Fobs and Fcalc are the observed and calculated structure factor amplitudes, respectively.
[b] R_{free} was calculated as R_{work} using a randomly selected subset of unique reflections not used for structural refinement.

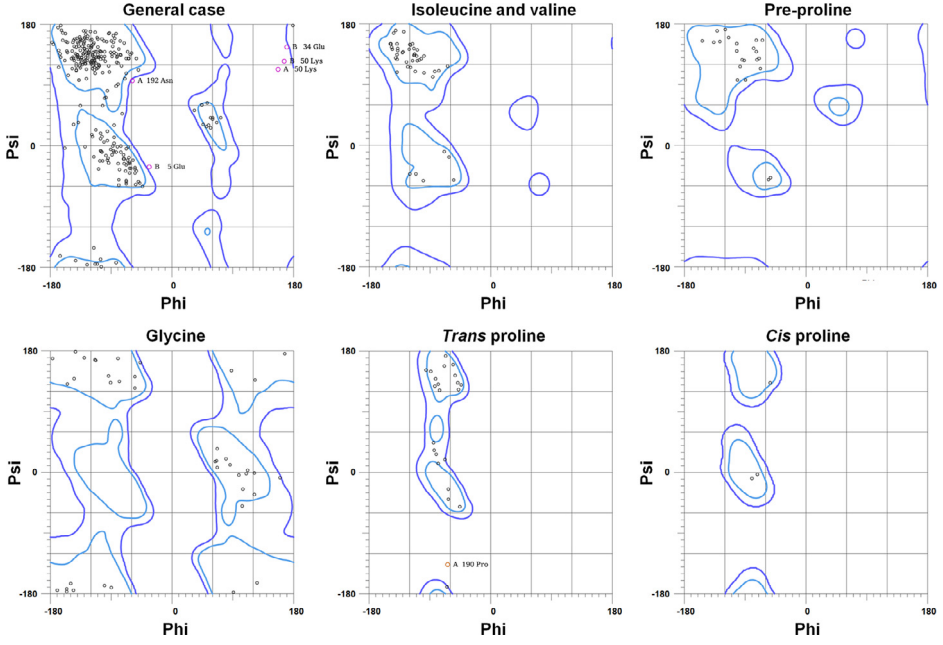

Fig. 2. Ramachandran plot of the deposited crystal structure of mDsRed.

The crystal structure of mDsRed exhibited the β-barrel fold (Fig. 3A). The mDsRed chromophore, generated by post-translational modification of the Gln66-Tyr67-Gly68 tripeptide, is almost at the center of the β-barrel fold (Fig. 3B). The surface structure of mDsRed showed that the mDsRed-B molecule exhibited a solvent-accessible hole with ~3.80 Å diameter between the β7 and β10 strands, which connects with the chromophore, whereas no accessible hole was observed in the mDsRed-A molecule, indicating that the residues near the β7 and β10 strands were flexible. The observed hole in mDsRed-B is ~8.16 Å away from the hydroxyl group of the tyrosine ring in the chromophore.

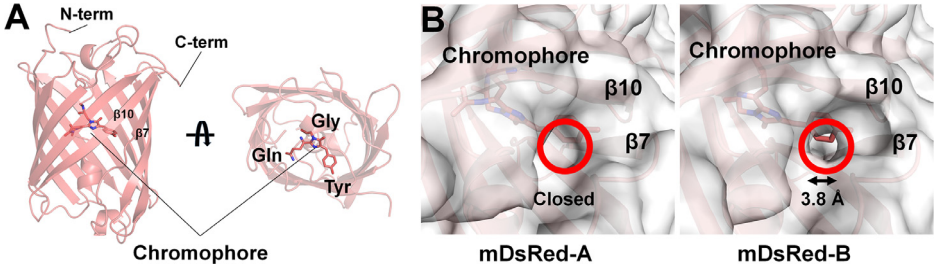

Fig. 3. Crystal structure of mDsRed. (A) Cartoon representation of mDsRed containing the chromophore comprising the tripeptide Gln66-Tyr67-Gly68. (B) Surface structure of mDsRed showing the hole between the $\beta 7$ and $\beta 10$ strands of mDsRed-B.

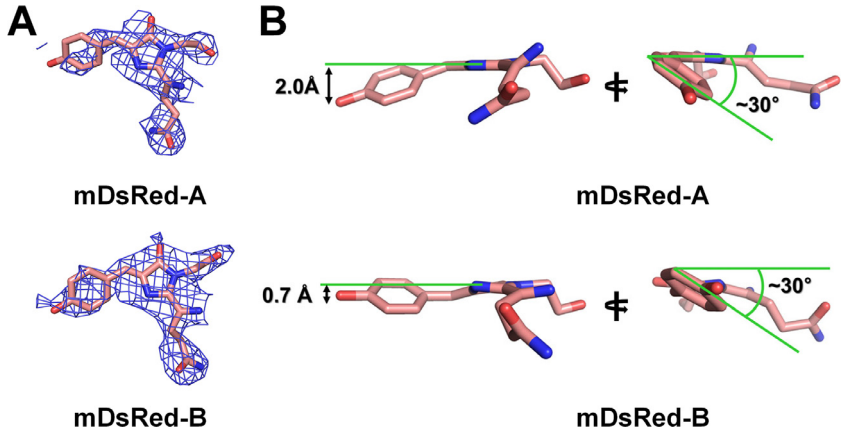

Fig. 4. Conformation of the mDsRed chromophore. (A) 2mFo-DFc (blue mesh, 0.8 σ) and mFo-DFc (green mesh, 3.0 σ and red mesh, -3.0 σ) electron density maps of the mDsRed chromophore. (B) Analysis of the configuration of the mDsRed chromophore. The figure was obtained from [1] and modified.

The electron density map of the β-barrel region containing the residues near the chromophore was observed, whereas the electron density map of the tyrosine-ring group in the chromophore was relatively poor (Fig. 4A), indicating the conformational flexibility of the mDsRed chromophore. The two mDsRed chromophores are in *cis*-configuration between the tyrosine- and imidazoline-ring groups. The side view of the chromophore showed a nonplanar configuration between the tyrosine- and imidazoline-ring groups in the mDsRed chromophore (Fig. 4B). The position of the tyrosine ring of mDsRed-A was moved and rotated to the bottom direction by 2.0 Å and 30°, respectively. The position of the tyrosine ring of mDsRed-B was moved and rotated to the bottom direction by 0.7 Å and 30°, respectively (Fig. 4B). mDsRed chromophores interacted with Pro63, Arg95, Ser146, His163, Ser197, and Glu215 (Table 3).

The B-factor putty representation showed that the β-barrel fold of mDsRed was rigid, whereas the N- and C-terminal regions exhibited high flexibility (Fig. 5A). B-factor analysis indicated that the loop containing Asp78 and Asp207 in mDsRed-A and that containing Pro186, Gln188, and Asp132 in mDsRed-B were relatively more flexible compared to β-barrel regions (Fig. 5B). Comparison of the B-factor and normalized B-factor values for mDsRed-A and mDsRed-B revealed distinct molecular flexibility, which may be attributed to the influence of crystal packing.

The coordinates and structure factors of mDsRed can be downloaded from the Protein Data Bank (PDB; https://www.rcsb.org/structure/8WGP) in the following formats: structure coordinates (PDBx/mmCIF, PDBML, PDB), XRD data (PDBx/mmCIF), and map coefficients (MTZ format).

Table 3
Interactions between the chromophore and its neighboring residues.

Chromophore (atom)	Residue (atom)	Distance (Å)	
		mDsRed-A	mDsRed-B
CRQ66 (OH)	Ser146 (OG)	2.49	2.29
	His163 (NE2)	3.89	3.26
	Ser197 (O)	3.49	3.44
CRQ66 (N2)	Pro63 (O)	3.49	3.79
	Glu215 (OE1)	3.18	3.26
CRQ66 (O2)	Arg95 (NH2)	3.14	2.99
CRQ66 (OE1)	Gln213 (NE2)	3.27	3.01

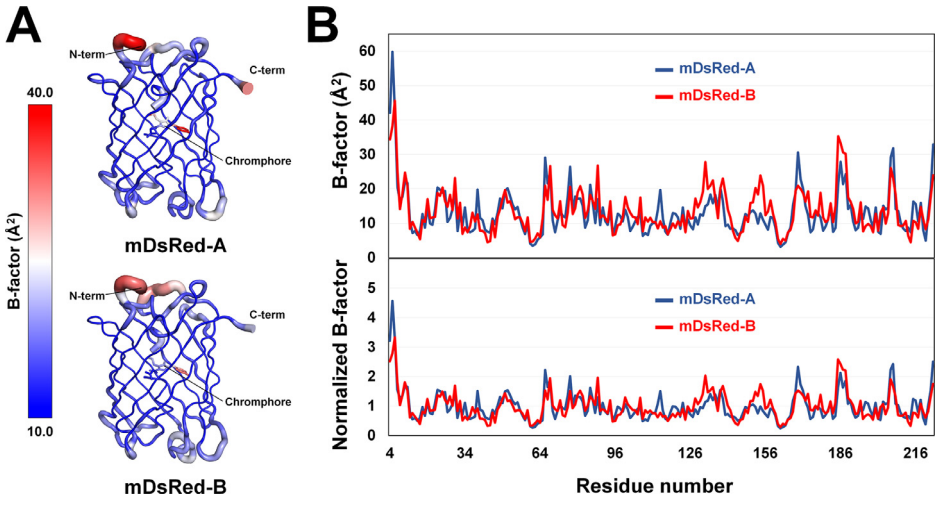

Fig. 5. Flexibility of mDsRed. (A) B-factor putty representation of mDsRed-A and mDsRed-B. (B) Profile of the B-factor and normalized B-factor for mDsRed-A (blue) and mDsRed-B (red).

The validation report (PDF, mmCIF) for the deposited mDsRed is also available for download. Additionally, information on data collection and structure determination has been deposited in the Protein Data Bank.

4. Experimental Design, Materials and Methods

The sample preparation, XRD data collection, and structure determination were reported previously [1]. Briefly, the pDsRed-Monomer vector containing mDsRed (catalog no. 632467; Takara, Shiga, Japan) was transformed into Escherichia coli BL21 (DE3). Cells were grown in an LB broth medium containing ampicillin (0.1 μg/mL) at 37°C until an OD_{600} of 0.5–0.6 was reached. Protein expression was induced by adding isopropyl β-D-thiogalactopyranoside. Cells were incubated at 20°C overnight and stored at 4°C for 1 day. After cell disruption by sonication, the mDsRed supernatant was purified by heat treatment and size exclusion chromatography. mDsRed (purity: 70–80 %) was crystallized using the sitting-drop vapor diffusion method at 18°C. mDsRed crystals were obtained using a crystallization solution containing 0.1 M bis-Tris (pH 5.5), 0.2 M magnesium chloride, and 25 % (w/v) polyethylene glycol 3,350. Rod-shaped mDsRed crystals ($10 \times 25 \times 200$ μm³) were obtained within 2 months and used for XRD data collection at the 7C beamline at the Pohang Light Source II (Republic of Korea) [12]. A mDsRed crystal was cryoprotected with a crystallization solution supplemented with 20 % (v/v) glycerol for 10 s. XRD

data were collected at 100 K, recorded on a Pilatus 6M detector (DECTRIS, Baden, Switzerland), and processed with the HKL2000 program [12]. The electron density map was obtained using the molecular replacement method with MOLREP (version 11.2.08) [13] implemented in CCP4 [14]. Structure building was performed using COOT (version 0.9.6) [15]. The model structure was refined with REFMAC5 (version 5.8.0267) [16] implemented in CCP4 [14]. The model structure was evaluated with MolProbity [17]. The structure factor and coordinate were deposited in the PDB (http://rcsb.org) under accession code 8WGP.

Limitations

Not applicable.

Ethics Statement

This work meets the ethical requirements for publication in this journal. This work does not involve human subjects, animal experiments, or any data collected from social media.

Data Availability

Crystal structure of DsRed-Monomer (Original data) (Protein Data Bank).

CRediT Author Statement

Ki Hyun Nam: Conceptualization, Methodology, Formal analysis, Investigation, Writing – original draft.

Acknowledgements

We would like to thank the beamline staffs at the 11C beamline at the Pohang Light Source II for their assistance with data collection. This work was funded by the National Research Foundation of Korea (NRF) (NRF-2021R1I1A1A01050838).

Declaration of Competing Interest

The authors declare that they have no known competing financial interests or personal relationships that could have appeared to influence the work reported in this paper.

References

[1] K.H. Nam, Structural flexibility of the monomeric red fluorescent protein DsRed, Crystals 14 (1) (2024) 62, doi:10.3390/cryst14010062.
[2] R.Y. Tsien, The green fluorescent protein, Annu. Rev. Biochem. 67 (1998) 509–544, doi:10.1146/annurev.biochem.67.1.509.
[3] R. Bizzarri, C. Arcangeli, D. Arosio, F. Ricci, P. Faraci, F. Cardarelli, F. Beltram, Development of a novel GFP-based ratiometric excitation and emission pH indicator for intracellular studies, Biophys. J. 90 (9) (2006) 3300–3314, doi:10.1529/biophysj.105.074708.
[4] I.J. Kim, S. Kim, J. Park, I. Eom, S. Kim, J.H. Kim, S.C. Ha, Y.G. Kim, K.Y. Hwang, K.H. Nam, Crystal structures of Dronpa complexed with quenchable metal ions provide insight into metal biosensor development, FEBS Lett. 590 (17) (2016) 2982–2990, doi:10.1002/1873-3468.12316.

[5] I.J. Kim, Y. Xu, K.H. Nam, Metal-induced fluorescence quenching of photoconvertible fluorescent protein DendFP, Molecules 27 (9) (2022) 2922, doi:10.3390/molecules27092922.
[6] K.H. Nam, Fluorescent protein-based metal biosensors, Chemosensors 11 (4) (2023) 216, doi:10.3390/chemosensors11040216.
[7] M.V. Matz, A.F. Fradkov, Y.A. Labas, A.P. Savitsky, A.G. Zaraisky, M.L. Markelov, S.A. Lukyanov, Fluorescent proteins from nonbioluminescent Anthozoa species, Nat. Biotechnol. 17 (10) (1999) 969–973, doi:10.1038/13657.
[8] B.J. Bevis, B.S. Glick, Rapidly maturing variants of the Discosoma red fluorescent protein (DsRed), Nat. Biotechnol. 20 (1) (2002) 83–87, doi:10.1038/nbt0102-83.
[9] R. Ranganathan, M.A. Wall, M. Socolich, The structural basis for red fluorescence in the tetrameric GFP homolog DsRed, Nat. Struct. Biol. 7 (12) (2000) 1133–1138, doi:10.1038/81992.
[10] D.E. Strongin, B. Bevis, N. Khuong, M.E. Downing, R.L. Strack, K. Sundaram, B.S. Glick, R.J. Keenan, Structural rearrangements near the chromophore influence the maturation speed and brightness of DsRed variants, Protein Eng. Des. Sel. 20 (11) (2007) 525–534, doi:10.1093/protein/gzm046.
[11] T.S. Hawley, W.G. Telford, A. Ramezani, R.G. Hawley, Four-color flow cytometric detection of retrovirally expressed red, yellow, green, and cyan fluorescent proteins, BioTechniques 30 (5) (2001) 1028–1034, doi:10.2144/01305rr01.
[12] S.Y. Park, S.C. Ha, Y.G. Kim, The protein crystallography beamlines at the pohang light source II, Biodesign 5 (1) (2017) 30–34.
[13] A. Vagin, A. Teplyakov, Molecular replacement with MOLREP, Acta Crystallogr. D Biol. Crystallogr. 66 (Pt 1) (2010) 22–25, doi:10.1107/S0907444909042589.
[14] J. Agirre, M. Atanasova, H. Bagdonas, C.B. Ballard, A. Baslé, J. Beilsten-Edmands, R.J. Borges, D.G. Brown, J.J. Burgos-Mármol, J.M. Berrisford, P.S. Bond, I. Caballero, L. Catapano, G. Chojnowski, A.G. Cook, K.D. Cowtan, T.I. Croll, J.É. Debreczeni, N.E. Devenish, E.J. Dodson, T.R. Drevon, P. Emsley, G. Evans, P.R. Evans, M. Fando, J. Foadi, L. Fuentes-Montero, E.F. Garman, M. Gerstel, R.J. Gildea, K. Hatti, M.L. Hekkelman, P. Heuser, S.W. Hoh, M.A. Hough, H.T. Jenkins, E. Jiménez, R.P. Joosten, R.M. Keegan, N. Keep, E.B. Krissinel, P. Kolenko, O. Kovalevskiy, V.S. Lamzin, D.M. Lawson, A.A. Lebedev, A.G.W. Leslie, B. Lohkamp, F. Long, M. Malý, A.J. McCoy, S.J. McNicholas, A. Medina, C. Millán, J.W. Murray, G.N. Murshudov, R.A. Nicholls, M.E.M. Noble, R. Oeffner, N.S. Pannu, J.M. Parkhurst, N. Pearce, J. Pereira, A. Perrakis, H.R. Powell, R.J. Read, D.J. Rigden, W. Rochira, M. Sammito, F. Sánchez Rodríguez, G.M. Sheldrick, K.L. Shelley, F. Simkovic, A.J. Simpkin, P. Skubak, E. Sobolev, R.A. Steiner, K. Stevenson, I. Tews, J.M.H. Thomas, A. Thorn, J.T. Valls, V. Uski, I. Usón, A. Vagin, S. Velankar, M. Vollmar, H. Walden, D. Waterman, K.S. Wilson, M.D. Winn, G. Winter, M. Wojdyr, K. Yamashita, The CCP4 suite: integrative software for macromolecular crystallography, Acta Crystallogr. D Struct. Biol. 79 (6) (2023) 449–461, doi:10.1107/s2059798323003595.
[15] A. Casañal, B. Lohkamp, P. Emsley, Current developments in Coot for macromolecular model building of electron cryo-microscopy and crystallographic data, Protein Sci. 29 (4) (2020) 1055–1064, doi:10.1002/pro.3791.
[16] G.N. Murshudov, P. Skubak, A.A. Lebedev, N.S. Pannu, R.A. Steiner, R.A. Nicholls, M.D. Winn, F. Long, A.A. Vagin, REFMAC5 for the refinement of macromolecular crystal structures, Acta Crystallogr. D Biol. Crystallogr. 67 (Pt 4) (2011) 355–367, doi:10.1107/S0907444911001314.
[17] C.J. Williams, J.J. Headd, N.W. Moriarty, M.G. Prisant, L.L. Videau, L.N. Deis, V. Verma, D.A. Keedy, B.J. Hintze, V.B. Chen, S. Jain, S.M. Lewis, W.B. Arendall 3rd, J. Snoeyink, P.D. Adams, S.C. Lovell, J.S. Richardson, D.C. Richardson, MolProbity: more and better reference data for improved all-atom structure validation, Protein Sci. 27 (1) (2018) 293–315, doi:10.1002/pro.3330.